TRANSITION MEASUREMENTS IN A LAMINAR SUPERSONIC JET

By

CHARLES JEFFERSON MCCOLGAN II

Bachelor of Science

Oklahoma State University

Stillwater, Oklahoma

1972

Submitted to the Faculty of the Graduate College
of the Oklahoma State University
in partial fulfillment of the requirements
for the Degree of
MASTER OF SCIENCE
July, 1973

TRANSITION MEASUREMENTS IN A LAMINAR SUPERSONIC JET

Thesis Approved:

Dennis K McLaughlin
Thesis Adviser

Ladislaus J. Fila

William A. Seidelmann, Jr.

D D Durham
Dean of the Graduate College

PREFACE

This study is concerned with an investigation in a supersonic free jet. The purposes of the study were to determine the range of Reynolds number for which the jet is laminar, and to characterize the fluctuations in the jet (whether it was laminar or turbulent). The hot-wire anemometer was used for this investigation, with the Reynolds and Mach numbers of the jet being found through Pitot and static pressure measurements made at various locations in the facility. Some similarities between the results of this work and that done by other investigators in the laminar supersonic wake are noted.

The author wishes to express his appreciation to his major advisor, Dr. Dennis K. McLaughlin, and to his other committee members, Dr. W. G. Tiederman and Dr. L. J. Fila, for their advice and guidance concerning this work. Appreciation is also expressed to Mr. Gerry Morrison, who aided in the construction of the silicone oil manometer and Pitot probe employed in this study, and also aided in the reduction of the pressure data. A note of thanks is also given to Mr. Tim Troutt, who aided in the hot-wire data collection and reduction and for his help in the preparation of some of the figures.

Finally, the author would like to recognize the financial support of the National Science Foundation, whose grant number GK-32686 made this study possible.

TABLE OF CONTENTS

Chapter		Page
I.	INTRODUCTION	1
II.	EXPERIMENTAL INVESTIGATION	6
	Equipment	6
	Experimental Procedure	12
III.	EXPERIMENTAL RESULTS AND CONCLUSIONS	17
IV.	SUMMARY	41
SELECTED BIBLIOGRAPHY		43

LIST OF TABLES

Table | Page

I. Parameters for the Hot-Wire Measurements Consisting of Spectra and Spatial Amplitude Distributions of the Hot-Wire Fluctuations for Six Test Conditions 4

LIST OF FIGURES

Figure		Page
1.	Schematic of the Free Jet Test Section.	7
2.	Detail Drawing of the Hot-Wire Probe (Full Scale).	11
3.	Circuit Diagram of the Voltage Divider System	14
4.	Jet Centerline Mach Number as a Function of Nozzle Stagnation Pressure, with Representative Uncertainty Limits Shown	18
5.	Jet Centerline Mach Number at x/d = 2 as a Function of the Pressure Balance Condition Described by r_b, with Representative Uncertainty Limits Shown	20
6.	RMS Amplitude of Hot-Wire Voltage Fluctuations (Horizontal Scale, 31 mv/in or 12.2 mv/cm) Plotted Against Radial Position in the Jet (Vertical Axis) for Several Downstream Locations; $Re_d = 1.23 \times 10^4$, $r_b = 1.04$ (Ideally Expanded Jet)	22
7.	RMS Amplitude of Hot-Wire Voltage Fluctuations (Horizontal Scale, 234 mv/in or 92.1 mv/cm) Plotted Against Radial Position in the Jet (Vertical Axis) for Several Downstream Locations; $Re_d = 2.47 \times 10^4$, $r_b = 1.03$ (Ideally Expanded Jet)	23
8.	RMS Amplitude of Hot-Wire Voltage Fluctuations (Horizontal Scale, 234 mv/in or 92.1 mv/cm) Plotted Against Radial Position in the Jet (Vertical Axis) For Several Downstream Locations; $Re_d = 3.70 \times 10^4$, $r_b = 1.04$ (Ideally Expanded Jet)	24

Figure Page

9. Maximum Normalized RMS Fluctuation Level in the Shear Annulus as a Function of Downstream Position for the Ideally Expanded Jet at Three Reynolds Numbers 26

10. Normalized RMS Fluctuation Level on the Jet Centerline as a Function of Downstream Position for the Ideally Expanded Jet at Three Reynolds Numbers 28

11. RMS Amplitude of Hot-Wire Voltage Fluctuations (Horizontal Scale, 31 mv/in or 12.2 mv/cm) Plotted Against Radial Position in the Jet (Vertical Axis) for Several Downstream Locations; $Re_d = 1.23 \times 10^4$; $r_b = 1.85$ (Under Expanded Jet). 30

12. Frequency Spectrum of Hot-Wire Fluctuations in the Maximum Fluctuation Region of the Shear Annulus; $Re_d = 2.47 \times 10^4$, $r_b = 1.03$, $x/d = 4$, $r/d = 0.8$ 32

13. Frequency Spectrum of Hot-Wire Fluctuations in the Maximum Fluctuation Region of the Shear Annulus; $Re_d = 2.47 \times 10^4$, $r_b = 1.03$, $x/d = 4$, $r/d = 0.8$ 33

14. Frequency Spectrum of Hot-Wire Fluctuations in the Maximum Fluctuation Region of the Shear Annulus; $Re_d = 3.70 \times 10^4$, $r_b = 1.04$, $x/d = 3.5$, $r/d = 0.8$. 34

15. Frequency Spectrum of Hot-Wire Fluctuations in the Maximum Fluctuation Region of the Shear Annulus; $Re_d = 1.23 \times 10^4$, $r_b = 1.84$, $x/d = 5$, $r/d = 0.9$ 37

16. Frequency Spectrum of Hot-Wire Fluctuations in the Maximum Fluctuation Region of the Shear Annulus; $Re_d = 2.47 \times 10^4$, $r_b = 1.84$, $x/d = 4$, $r/d = 1.0$ 38

17. Frequency Spectrum of Hot-Wire Fluctuations in the Maximum Fluctuation Region of the Shear Annulus; $Re_d = 3.70 \times 10^4$, $r_b = 1.84$, $x/d = 3.5$, $r/d = 0.95$ 39

NOMENCLATURE

d	nozzle exit diameter
e'	RMS amplitude of the fluctuation component of the hot-wire bridge voltage
E	mean hot-wire bridge voltage
f	frequency
f_c	characteristic frequency of jet given by the ratio V_{jet}/d
M	Mach number
p_b	nozzle back pressure (test chamber pressure)
p_n	nozzle exit pressure
p_o	stagnation pressure measured upstream of the nozzle
p_p	pressure measured by the Pitot probe
r	radial position in the jet measured from the centerline
r_b	Pressure balance ratio described by p_n/p_b
Re_d	Reynolds number based on the nozzle exit diameter
St	Strouhal number, the non-dimensional frequency given by the ratio f/f_c
V_{jet}	centerline jet exit velocity calculated from isentropic relationships for compressible flow
x	axial distance from the nozzle exit

CHAPTER I

INTRODUCTION

In recent years noise pollution has received considerable attention from legislators. In particular, jet aircraft are being subjected to ever more stringent noise requirements. Although significant progress in reducing jet engine noise has been made, further investigation along these lines is needed.

Jet engine noise is made up primarily of two distinct components: noise from the bladed passages in the compressor and turbine and noise produced by the exhaust jet of hot gases. The noise production process in the compressor and turbine is mainly the result of the passage of the rotor blades by the stator blades at regular intervals, with a resulting almost pure tone noise. A combination of proper blade spacings and the use of acoustic absorption material in the inlet nacelle has proved very effective in reducing this type of noise. Reductions in the noise of the exhaust jet are much more difficult to achieve, with the only effective method being to reduce the exhaust velocity. Some techniques (such as a multiple exhaust nozzle) provide marginal noise reductions, but are not adequate to meet forthcoming standards. When the compressor and turbine noise are reduced by proper engine

design the exhaust noise may become predominant, necessitating effective treatment of this noise source.

Recently, jet noise investigators (1, 2) have theorized that a substantial portion of the exhaust noise is produced by large-scale fluctuations in the jet which are similar to instability waves in a laminar supersonic jet. In fact, Tam (3) based a theoretical investigation of the acoustic waves radiated by a turbulent supersonic jet on a small-disturbance theory derived on the basis of an assumption that shear layer instability is the dominating factor in the radiation of orderly acoustic waves from the region of the jet very close to the nozzle exit.

The theory is intended to predict the orientation of the radiated wave fronts with respect to the jet axis and was compared to experimental results he obtained for cold jets and a simulation of the heated exhaust of a jet engine (accomplished by operating a jet of helium into air). His results indicate close agreement between predicted and experimentally measured wave propagation angles, and support the idea that the shear layer instability is dominant in the physical process. However, this radiation constitutes only a small proportion of the total noise produced by the jet. The major noise production mechanism in the jet involves the presence of a large-scale instability in the jet core. This mode of jet instability closely resembles the large-scale instability of a laminar jet. With shear-layer instability theories yielding good results, the possibility that further stability theories could yield valuable information about the jet core fluctuation becomes apparent.

However, an experimental investigation in a turbulent jet is complicated by the presence of turbulence in the flow, which increases the difficulty of determining the characteristics of the jet. In the laminar jet, deterministic measurements can be made, resulting in much simpler data reduction. For the above reasons a complete stability analysis of a laminar supersonic jet has been undertaken.

The first step in a stability investigation is a transition analysis, which determines the limits of laminar flow in the jet. The objectives of the author's work were to develop a facility capable of producing a free laminar supersonic jet and to determine some of the flow characteristics of the jet. These objectives entailed developing good control over the pressures throughout the test facility and adequate pressure instrumentation. The investigation was carried out using the hot-wire anemometer, a technique which has previously been employed in many stability and transition studies (see for example (4), (5) and (6)).

It might be noted that the scarcity of information concerning transition in the laminar supersonic jet is somewhat alleviated by the information available from investigations of the laminar supersonic wake, which has characteristics somewhat similar to a laminar supersonic jet. These points are discussed at greater length in the following chapters.

The scope of the investigation of the jet flow included determination of the jet Reynolds and Mach numbers from the pressure data, and determination of the laminar or turbulent character of the jet from

the hot-wire measurements. The hot-wire measurements consisted of spatial amplitude distributions of the hot-wire fluctuations and frequency spectra of the fluctuations at a point in the jet. These measurements were made for three Reynolds numbers at two pressure balance conditions for each Reynolds number (see Table 1).

TABLE I

PARAMETERS FOR THE HOT-WIRE MEASUREMENTS CONSISTING OF SPECTRA AND SPATIAL AMPLITUDE DISTRIBUTIONS OF THE HOT-WIRE FLUCTUATIONS FOR SIX TEST CONDITIONS

Run	Reynolds Number	Pressure Balance, $r_b = p_n / p_b$
1	1.23×10^4	1.04
2		1.85
3	2.47×10^4	1.03
4		1.84*
5	3.70×10^4	1.04
6		1.84*

*Spatial amplitude distributions of RMS hot-wire fluctuations were not included for these two cases for reasons discussed in Chapter 3.

These measurements were sufficient to describe the behavior of the jet, and the results and conclusions of the investigation are presented in Chapter 3.

CHAPTER II

EXPERIMENTAL INVESTIGATION

Equipment

The current research is being carried out in the free-jet test section of the Oklahoma State University high-speed wind tunnel for a jet of nominal Mach number 2.65. The tunnel is operated by evacuating its downstream section and maintaining the stagnation pressure at 14.7 psia (76.0 cm Hg) or less, with the result that the jet exhausts into an ambient pressure of 0.675 psia (3.52 cm Hg) or less in the test section (see Figure 1). This procedure is used so that a low jet Reynolds number may be obtained in contrast to the research of other investigators (for example, see Nagamatsu (7), who exhausted the jet to atmospheric pressure). The Reynolds number of the jet under consideration is hence at least a factor of 20 lower than those investigated previously.

The inlet to the tunnel consists of a stilling section which admits room air to the facility at a stagnation temperature of about 70°F (21°C). The stilling section provides for reduction of turbulence and control of the stagnation pressure to the nozzle. A diaphragm valve at the inlet affords precise control over the flow rate and hence over

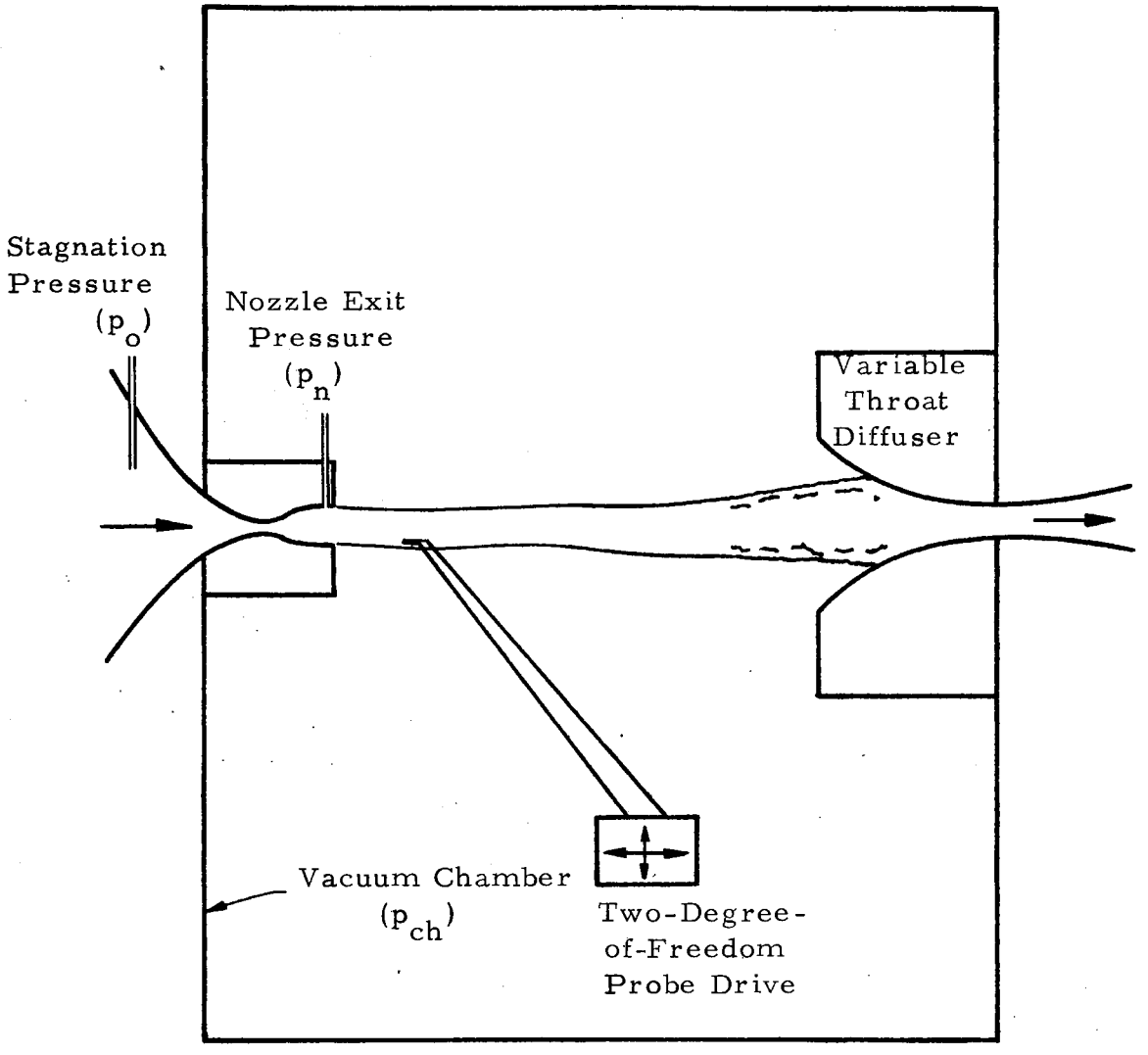

Figure 1. Schematic of the Free Jet Test Section

the stagnation pressure. Following the valve is an adapter to the large diameter (6 inches; 15.24 cm.) quieting section. Flow through the adapter impinges on a plate mounted in the stilling section, with the air flowing through 32 evenly distributed 3/16 inch (0.48 cm.) holes in the plate. The purpose of the plate is to distribute the flow more evenly over the cross-section of the stilling section. Following the plate, reduction of turbulence is obtained through a two-inch (5.08 cm.) thick section of foam rubber, which precedes six progressively finer screens spaced two inches (5.08 cm.) apart. The last screen is at a distance of 10 inches (25.4 cm.) from the nozzle throat, allowing time for the small-scale distrubances it introduces to dissipate before reaching the nozzle.

The nozzle is a converging-diverging axisymmetric nozzle, with a throat diameter of 0.215 inches (5.46 mm.) and an exit diameter of 0.375 inches (9.52 mm.). The calculated area ratio A/A^* is 3.036, which yields a nominal Mach number of 2.65. The distance from the throat to the exit plane is two inches (5.08 cm.), and the walls are cut straight, with a resulting included divergence angle of 4.58 degrees. The nozzle had a simple conical exit section rather than a contoured section for several reasons. First, it was much easier to construct than a contoured nozzle would have been. Second, in order to get parallel flow from a contoured nozzle, a boundary layer calculation would have been necessary, but would have been valid for only one Reynolds number. The design was made with the knowledge that the

nozzle would be operated over a range of Reynolds numbers. Finally, the flow is seen to deviate only slightly from parallel because the divergence of the nozzle is small. Note that the ratio of the stilling section area to nozzle exit area (or the contraction ratio) is 256 to 1, a factor which tends to further diminish the effect of any turbulence in the stilling section.

Downstream of the nozzle is a variable throat diffuser (see Figure 1) which allows precise control over the test chamber pressure. The diffuser is two-dimensional, with control being achieved by two flexible stainless steel bands which are operated by a crank mounted external to the test chamber. The chamber pressure p_b (back pressure for the nozzle) may be set so that the pressure balance ratio r_b (given by p_n/p_b where p_n is the nozzle exit pressure) results in any pressure balance condition desired. That is, for $r_b < 1$ the jet is over-expanded, while for $r_b = 1$ it is ideally expanded, and the jet is under-expanded for $r_b > 1$. Flow through the diffuser exhausts into a 12-inch (30.48 cm.) diameter pipe about 50 feet (15.23 m.) long, which leads to a 1,100 cubic foot (31.8 cubic meter) vacuum reservoir. The reservoir is evacuated by a Kinney vacuum pump having a capacity of 200 cfm (5,590 liters per minute). The large volume of the vacuum reservoir and associated piping minimizes any pressure fluctuations that could reach the test chamber from the vacuum pump. Vibration is minimized by the flexible piping which connects the vacuum pump and the reservoir. Thus the test chamber is effectively

isolated from vibration and pressure fluctuations. Another feature of the vacuum system is that it provides for continuous test runs.

Pressures throughout the wind tunnel are measured on two manometers, one with mercury as the working fluid and the other having DC 200 silicone oil as the working fluid. The stagnation pressure (p_o) and the Pitot pressure (p_p) are measured on the mercury manometer, while the nozzle exit pressure (p_n) and the test chamber pressure (p_b) are measured on the silicone manometer. The stagnation pressure (p_o) is taken at a static tap[1] in the stilling section downstream of the screens, while p_p is the pressure measured by a Pitot probe mounted on the probe drive. Nozzle exit pressure (p_n) is taken at a static tap less than 1/8 inch (3 mm.) from the jet exit, while p_b is taken at a static tap in the chamber wall. The manometer is used for p_n in order to get greater sensitivity and accuracy in these measurements and for good accuracy in determining r_b (defined as the ratio p_n/p_b). Both manometers were referenced to a vacuum of 10^{-5} psia (0.02 mm Hg) as measured by a Kinney type T.D. 2 vacuum guage.

Hot-wire measurements were made in order to investigate the

---

[1] Since the ratio of the cross-section area of the stilling section to the nozzle throat area is about 800, the velocity in the stilling section is about two feet per second. The difference between static pressure and total pressure will therefore be negligible at this point.

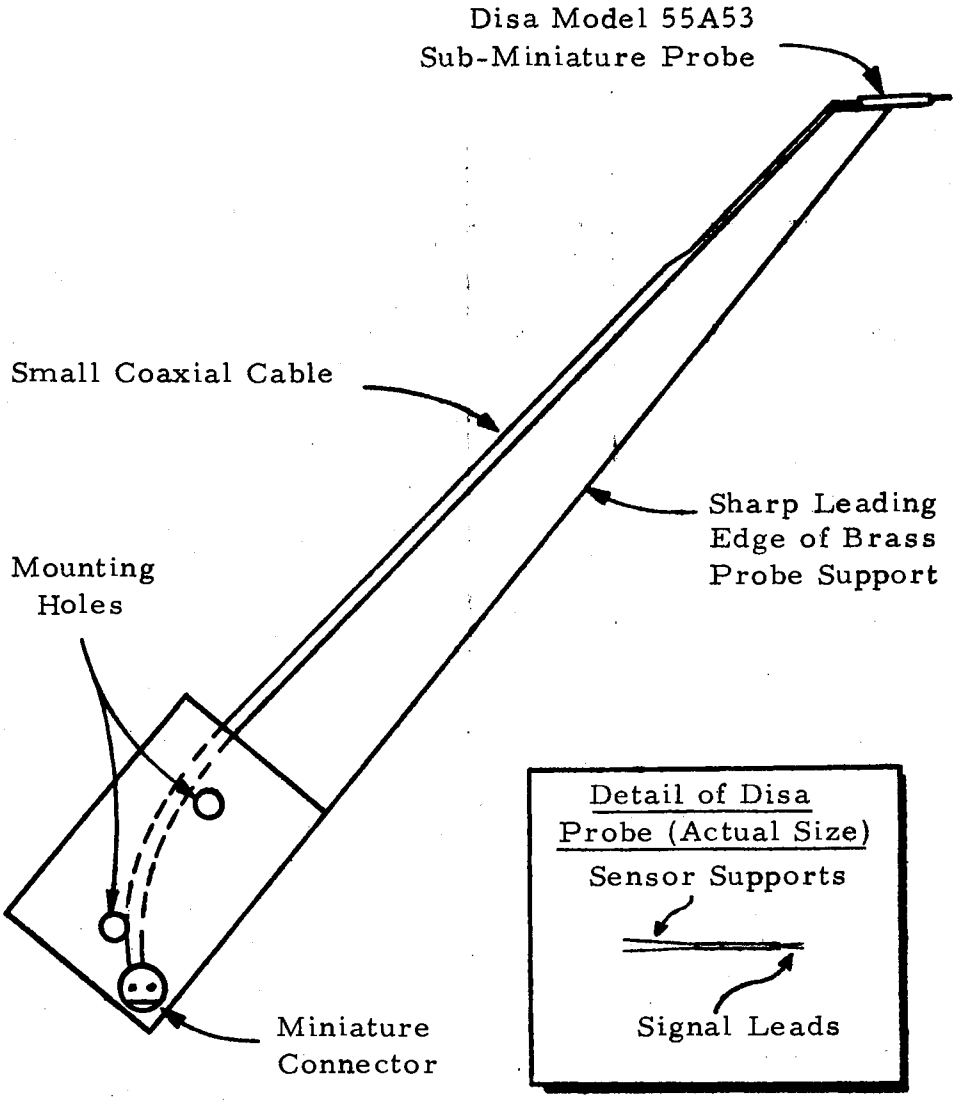

Probe Support Data

Included Wedge Angle:	8 Degrees
Maximum Wedge Thickness at Probe Location:	0.035 inch
Leading to Trailing Edge Length at Probe Location:	5/16 inch
Maximum Wedge Thickness:	0.065 inch
Vertical Wedge Height:	3.0 inches

Disa Model 55A53 Probe Data

Sensor Support Length:	3 mm
Sensor Length:	0.45 mm
Sensor Diameter:	5 microns
Sensor Material:	Platinum Plated Tungsten

Figure 2. Detail Drawing of the Hot-Wire Probe (Full Scale)

mean and fluctuating components of velocity[2] in the jet. These measurements were made with a Disa model 55A53 sub-miniature probe mounted on a brass wedge airfoil (see Figure 2). The probe is operated in the constant-temperature mode by the Disa model 55A01 Constant Temperature Anemometer. The anemometer provides outputs for the mean and fluctuating components of the hot-wire bridge voltage. Meters on the front of the anemometer indicate mean voltage and the root-mean-square intensity of the voltage fluctuations. Other equipment used in conjunction with the hot-wire anemometer include a Ballantine model 710A linear AC to DC converter, a Mosely model 2DX-Y plotter, and a Hewlett-Packard model 302A Wave Analyzer. The procedure for the use of this equipment is described in the next section.

Experimental Procedure

The transition process is largely delineated by spatial amplitude distribution measurements of the hot-wire voltage fluctuations. The spatial amplitude distribution is a record of the RMS fluctuation level as a function of probe position. These measurements were made with

---

[2] In supersonic flow the hot-wire is actually sensitive to velocity pressure, and temperature fluctuations in the jet. Finding the true velocity fluctuation levels is very difficult experimentally and mathematically, and is beyond the scope of this work. This detailed investigation is not necessary for a transition study, however, as only relative and not absolute fluctuation levels are needed for the analysis. As a result, the terms "velocity fluctuation" and "hot-wire bridge voltage fluctuation" may not be interchanged; and the distiction is kept in mind throughout this work.

the probe mounted on the two-degree-of freedom drive mechanism in the test chamber. The probe was operated at an overheat of 20 percent, which gave good sensitivity and long wire life. (The latter is important due to the difficulty involved in the repair of this small size probe.) The overheat was set by measuring the probe cold resistance (R_c), which was always found to be within 0.2% of 2.82 ohms, and then multiplying this value by 1.2 to get operating resistance (R_h). With R_h set on the anemometer, the correct overheat was maintained. The operating resistance for this overheat was 3.38 ohms, with a corresponding difference between the wire temperature and the stagnation temperature of the jet and the flow of 90°F. (50°C.) This operating temperature was maintained by the anemometer.

Plots of the RMS spatial distribution of hot-wire voltage fluctuation amplitude were made on the X-Y plotter. The Y axis of the plotter was driven by the output of a voltage divider system[3], with the vertical displacement on the plotter being proportioned to the vertical displacement of the probe from its reference position. The X-axis of the plotter was driven by a DC voltage proportional to the RMS hot-wire fluctuation

---

[3]The voltage divider consists of a linear (to 1 percent) 10,000 ohm ten-turn potentiometer which is driven through a gear reduction by the vertical screw drive on the probe drive. The exciter voltage is provided by a six volt heavy duty battery. Another voltage divider is placed in series with the above to allow zeroing of the output voltage with the probe in its reference position. (See Figure 3 for circuit diagram.) Use of the variable gain on the Y-axis of the plotter allowed any scale factor between vertical probe travel and pen motion to be set. (This was approximately 11 in all cases.)

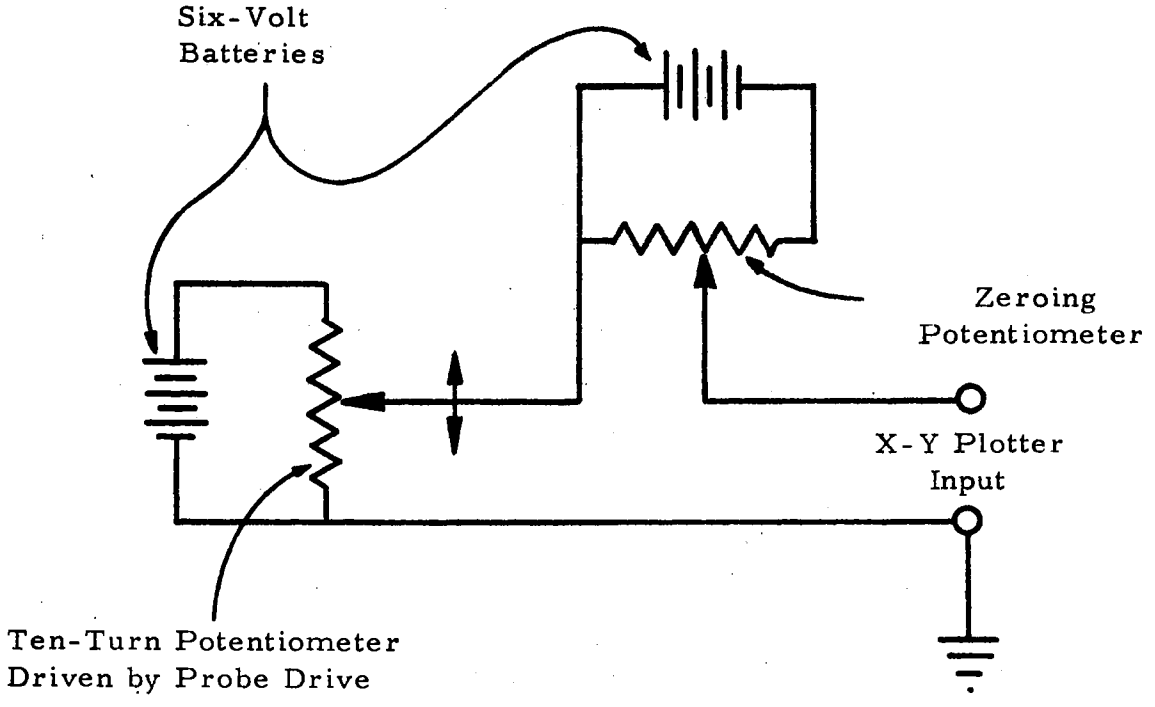

Figure 3. Circuit Diagram of the Voltage Divider System

voltage. The DC voltage was provided by passing the fluctuation signal from the anemometer through the Ballantine AC-DC converter. With this arrangement, driving the probe upward through the jet resulted in a continuous trace of RMS fluctuation level as a function of vertical position at a constant downstream location. The fact that the horizontal pen deflection was proportional to RMS fluctuation level was verified by recording the maximum and minimum fluctuation levels in the jet read from the RMS milli-volt meter on the anemometer to the maximum and minimum pen deflections. These were found to agree very well. Recording the mean bridge voltage along with the fluctuation level allowed estimation of the relative levels of turbulence in the jet. After each traverse the probe was moved downstream one jet diameter (3/8 inch or 0.952 cm.) and a new traverse made until the limit of the probe travel was reached (10 jet diameters). For each new traverse the reference point on the X-axis of the plotter was changed to prevent overlapping and confusion of the traces. The resulting system of plots depicts the behavior of the RMS fluctuation amplitude transverse to the jet and in the downstream direction.

Frequency spectra of the hot-wire voltage fluctuations give information which is very useful in determining whether or not the jet flow is laminar (in particular for the ideally expanded cases). They also provide interesting information concerning the behavior or turbulent jets for the under-expanded case. These phenomena are discussed at greater length in the following chapter.

Spectrum information was again obtained by employing the X-Y plotter. The input to the X-axis of the plotter was the voltage output of the Hewlett-Packard Sweep Drive, which is linearly proportioned to frequency of the Hewlett-Packard 302A Wave Analyzer. The suitably filtered[4] fluctuation voltage was the input to the Wave Analyzer, whose output drove the Y-axis of the plotter. Data were taken by positioning the probe at the desired location in the jet and, by means of the sweep drive, sweeping the Analyzer through the desired frequency range (0 to about 25,000 Hz). The frequency "window" of the wave analyzer (6 Hz) combined with the sweep rate of the drive (1000 Hz per minute) produced an "analyzing time" at any single frequency of 0.36 seconds. The resulting spectrum is not extremely accurate (due to the short averaging time) but it does show the major spectral components of the fluctuations at a point in the jet.

The hot-wire investigations were carried out for six jet cases (as described in Chapter 1). The pressures set in each case were based on the results of the Pitot probe measurements. The results of the pressure measurements and hot-wire investigation are discussed in the following chapter.

---

[4] Filter settings were 200 Hz for the high pass filter and 50,000 Hz for the low-pass filter. These settings prevented power supply noise or any electrical resonance in the probe-anemometer set-up (at about 100 kilo Hz) from appearing in the fluctuation output but did not interfere with any significant signals.

CHAPTER III

EXPERIMENTAL RESULTS AND CONCLUSIONS

Pitot and static pressure measurements were required in order to determine the Mach and Reynolds numbers of the jet. At a fixed Mach number, the Reynolds number is dependent only on the stagnation pressure of the jet (for constant stagnation temperature). When the jet Mach number is known, determining the jet Reynolds number is a straightforward task.

The experimentally determined Mach number on the jet centerline was based on the ratio of the Pitot pressure at the nozzle exit to the stagnation pressure[1], assuming isentropic flow through the nozzle. Figure 4 shows the variation in jet Mach number with stagnation pressure. These measurements were made with the Pitot probe located on the jet axis in the nozzle exit plane. This figure indicates that the jet centerline Mach number decreases with decreasing nozzle stagnation pressure, or decreasing Reynolds number. However, for the range of stagnation pressures used in the investigation, 1.98 psia to

---

[1] All Mach numbers determined on the basis of pressure or area ratio were found by means of using tables in Reference 8. Also, Reynolds numbers were calculated with the aid of Chart 25, page 69, in Reference 8.

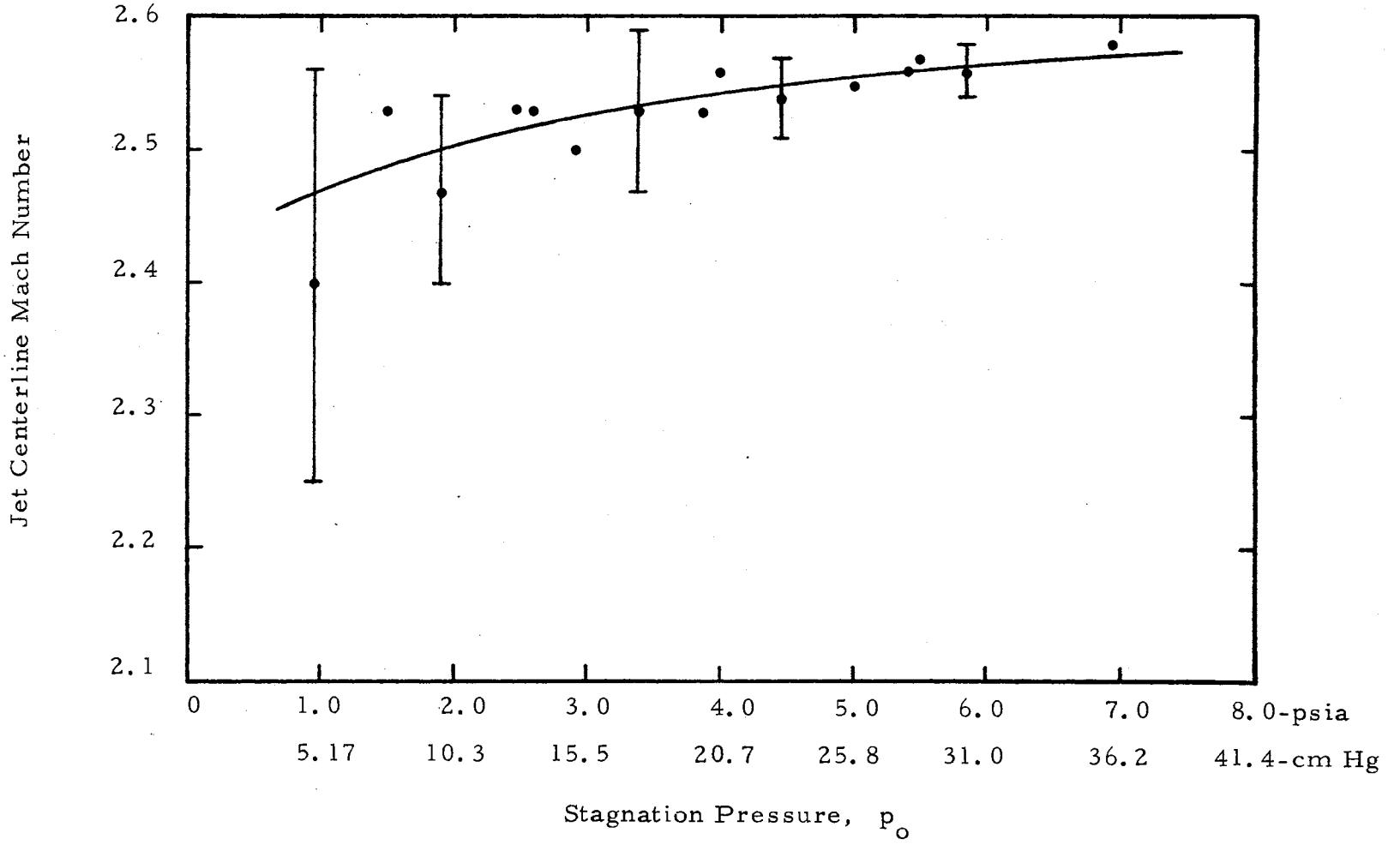

Figure 4. Jet Centerline Mach Number as a Function of Nozzle Stagnation Pressure, with Representative Uncertainty Limits Shown

5.93 psia (10.1 to 30.4 cm Hg), the jet Mach number is constant within about 2%. The variation in Mach number is probably due to variations in the boundary layer thickness with Reynolds number (as the Reynolds number decreases the boundary layer thickens), which would result in changes in the effective area ratio of the nozzle and a reduction in jet Mach number. This is not a very pronounced effect for the nozzle used, however.

An important factor in the behavior of the jet is the pressure balance condition described by the balance ratio r_b (ratio of nozzle exit pressure, p_n, to the back pressure in the test chamber, p_b). This ratio may be set so that the jet is over-expanded ($r_b > 1$), ideally expanded ($r_b \approx 1$), or under-expanded ($r_b > 1$). Figure 5 shows the variation in Mach numbers at x/d = 2 as a function of r_b for stagnation pressures of 1.98 and 9.88 psia (10.1 and 30.4 cm Hg). This figure indicates that an effective jet Mach number may be based on the ratio p_b/p_o, assuming the jet expands to the chamber pressure after exiting from the nozzle. For hot-wire measurements in the jet, two values of r_b were chosen; one for the ideally expanded jet ($r_b = 1.04$) and one for a highly under-expanded jet ($r_b = 1.84$, corresponding to an effective Mach number of 3.0 based on the ratio p_b/p_o).

The pressure balance ratio noted above for the ideally expanded case ($r_b = 1.04$) differs from the value of 1.00 which would be expected (the value of 1.04 was determined by trial and error). This discrepancy is due to the fact that p_n does not represent the true static pressure on

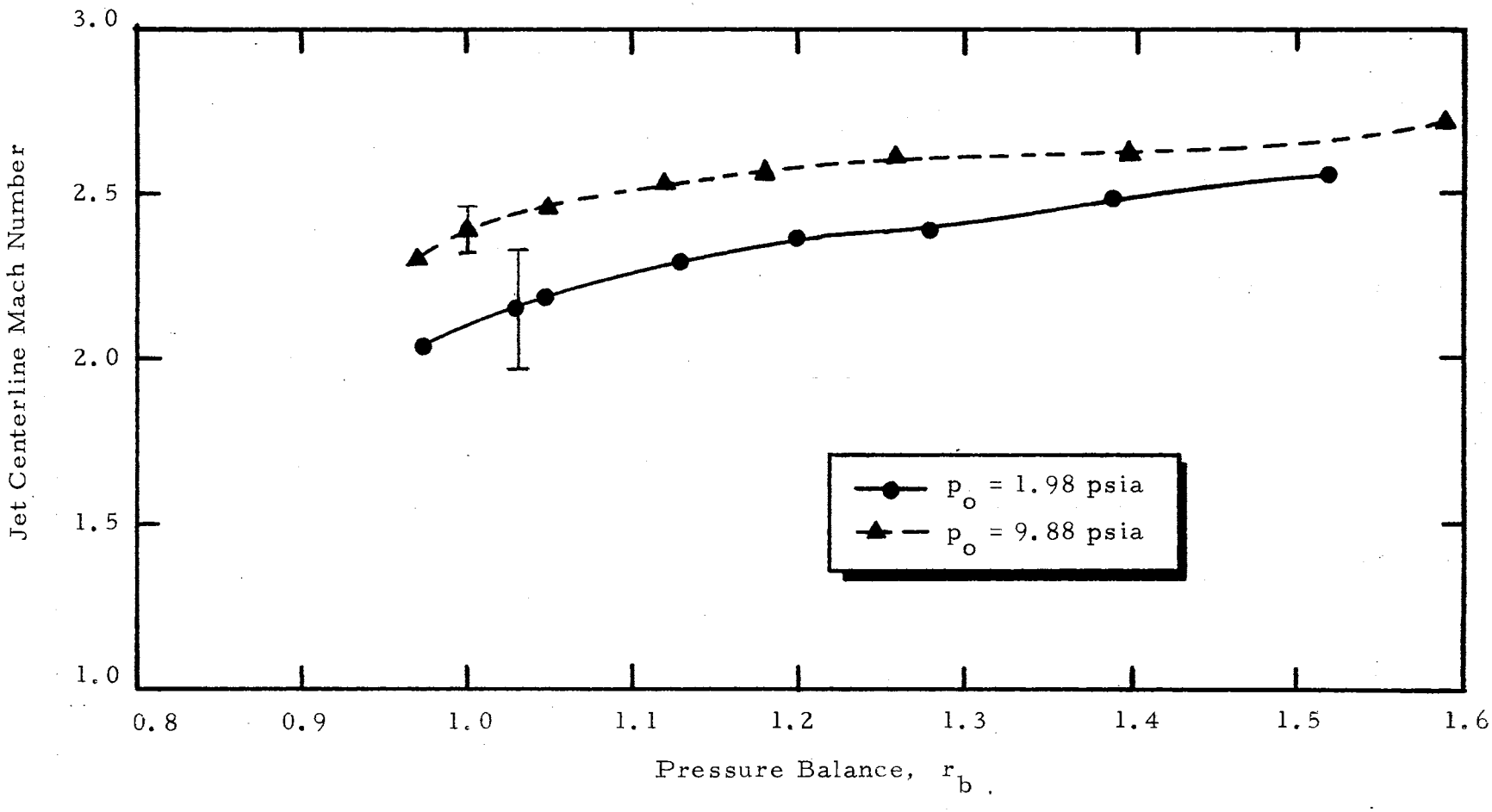

Figure 5. Jet Centerline Mach Number at x/d = 2 as a Function of the Pressure Balance Condition Described by r_b, with Representative Uncertainty Limits Shown

the axis of the nozzle at its exit, a conclusion which can be deducted for the following evidence. At a stagnation pressure of 5.9 psia (30.4 cm Hg), the jet Mach number calculated from the ratio p_p/p_o (see Figure 4) is 2.55 ± 0.02, while the Mach number based on the ratio p_n/p_o is 2.44 ± 0.02. Since Pitot pressure measurements are fairly insensitive to probe alignment errors, and since accurate static pressure measurements are sometimes very difficult, it was concluded that p_n was in error. This error could have been due to streamline curvature at the nozzle exit. Calculations indicate that a streamline radius of curvature of 0.37 in. (9.4 mm) would be sufficiently small to produce the observed difference between measured and theoretically calculated values of static pressure on the centerline at the nozzle exit. The actual cause is not known at the present time, however.

Figures 6, 7, and 8 are plots of the spatial amplitude distribution of RMS hot-wire voltage fluctuations in the ideally expanded jet for Reynolds numbers of 1.23×10^4, 2.47×10^4, and 3.70×10^4, respectively. It should be noted that the horizontal scale factors (corresponding to the RMS hot-wire fluctuation level) differ by a factor of about seven between Figures 6 and 7. The maximum fluctuation level in Figure 7 is actually about 30% higher than that in Figure 6, but is comparable to that of Figure 8 (the horizontal scale is the same for Figures 7 and 8).

In each figure (for the $x/d = 1$ profile) peaks in the RMS fluctuation amplitude occur at a radial position, r/d of about 0.5. These peaks

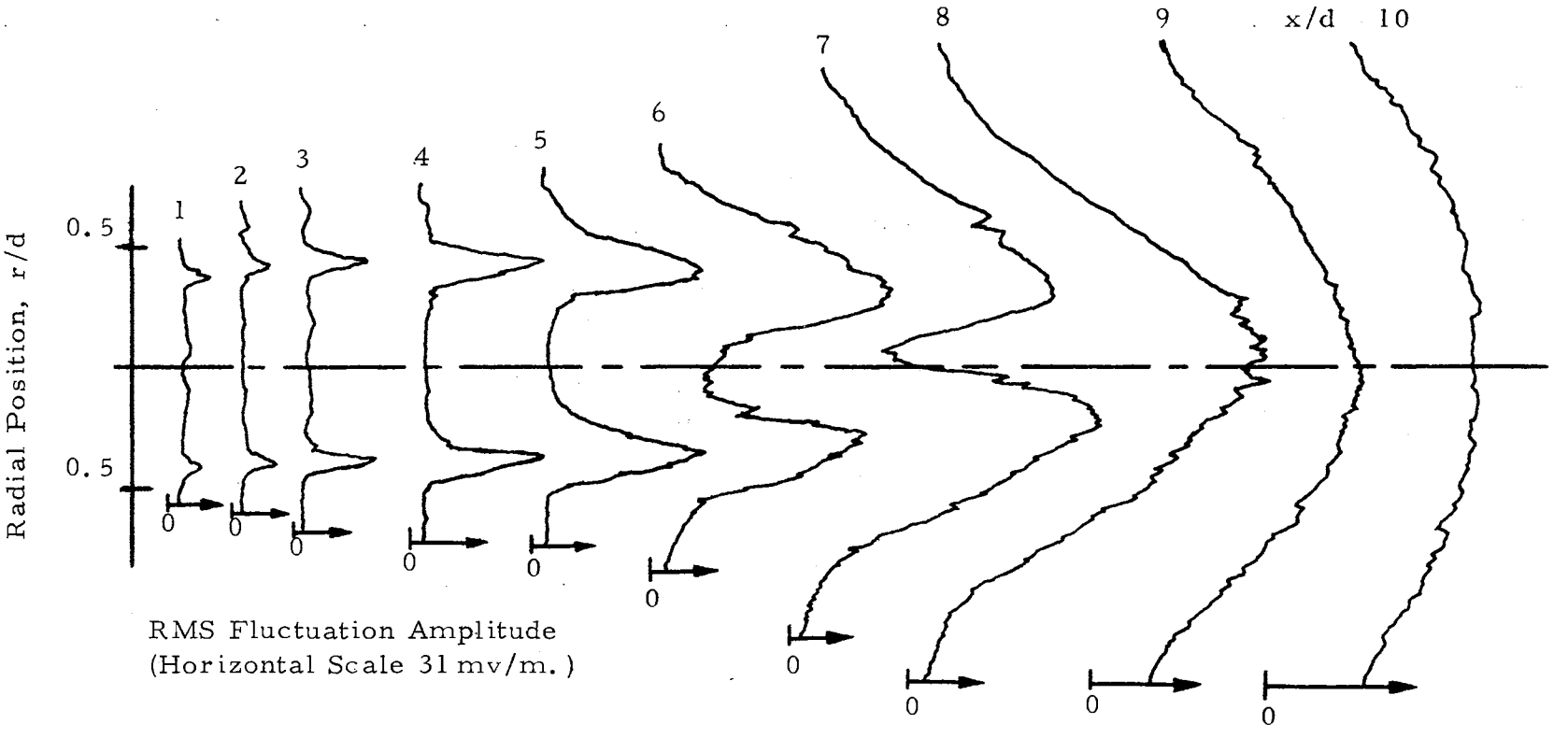

Figure 6. RMS Amplitude of Hot-Wire Voltage Fluctuations (Horizontal Scale, 31 mv/in or 12.2 mv/cm) Plotted Against Radial Position in the Jet (Vertical Axis) for Several Downstream Locations; $Re_d = 1.23 \times 10^4$, $r_b = 1.04$ (Ideally Expanded Jet)

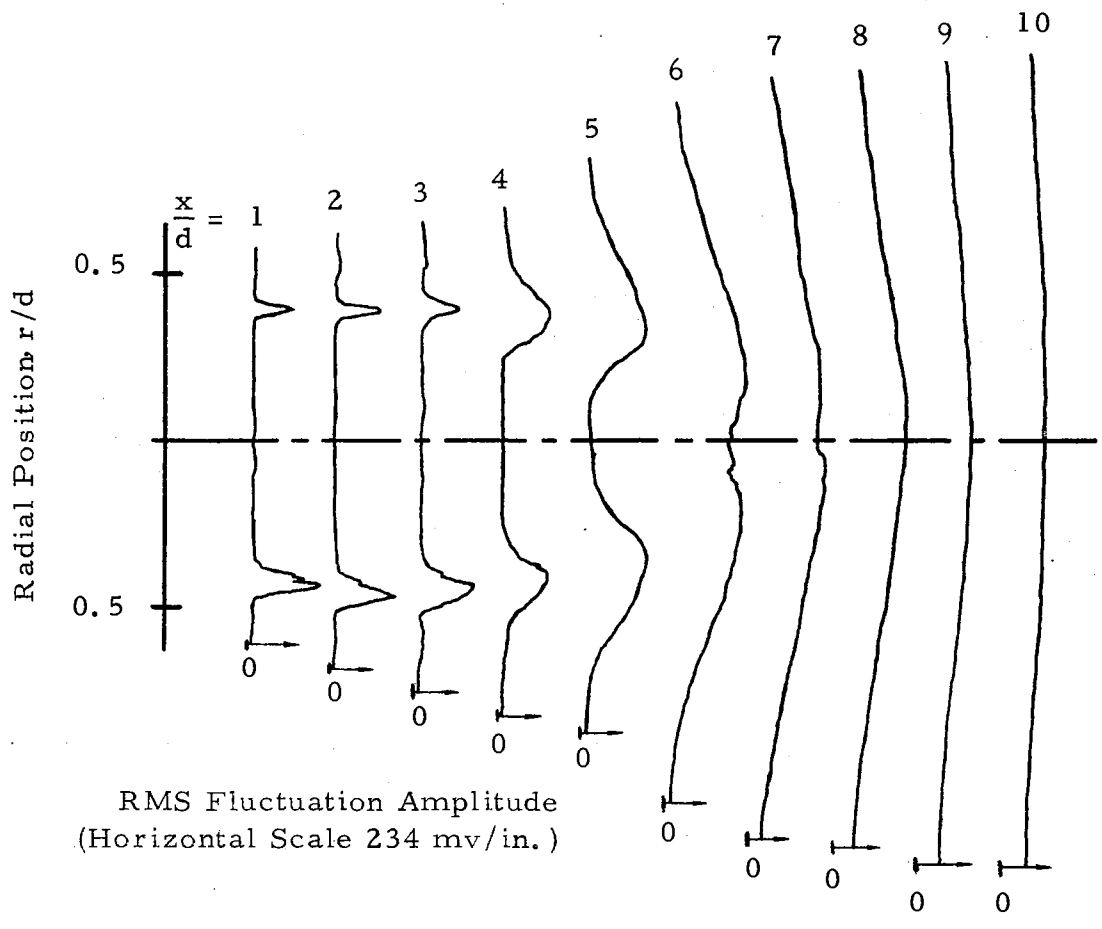

Figure 7. RMS Amplitude of Hot-Wire Voltage Fluctuations (Horizontal Scale, 234 mv/in or 92.1 mv/cm) Plotted Against Radial Position in the Jet (Vertical Axis for Several Downstream Locations; $Re_d = 2.47 \times 10^4$, $r_b = 1.03$ (Ideally Expanded Jet)

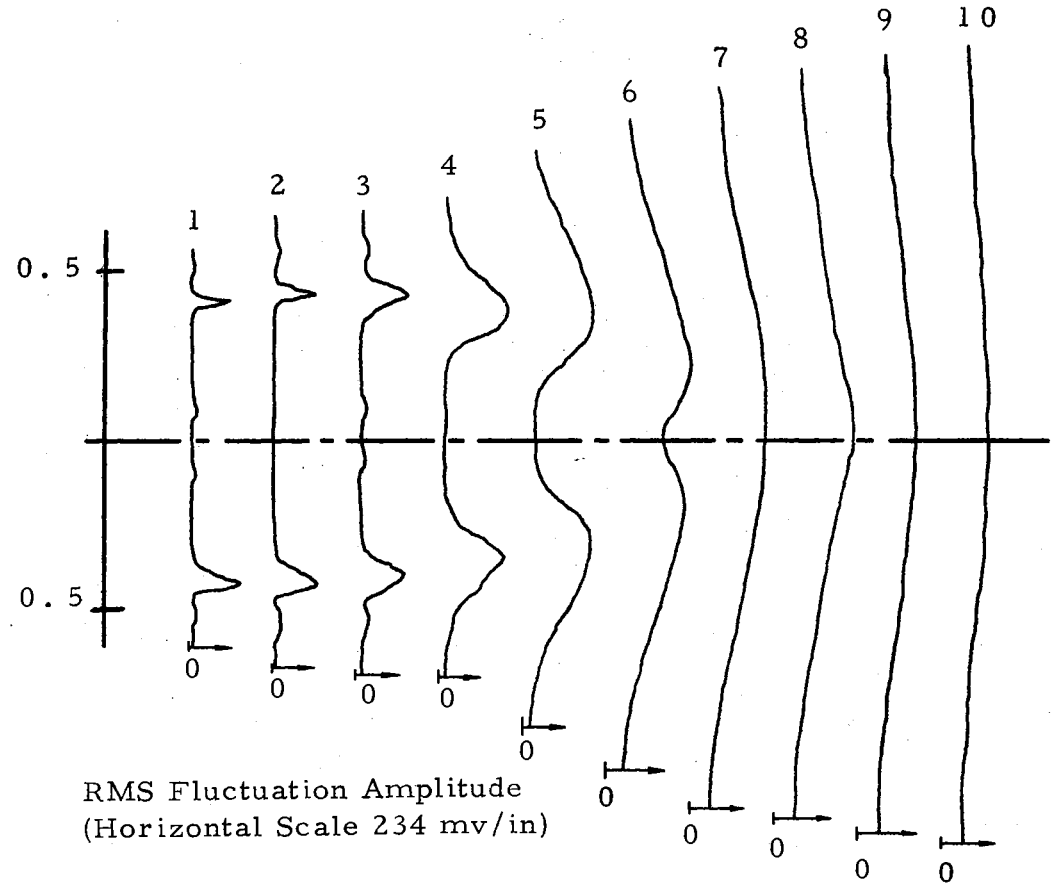

Figure 8. RMS Amplitude of Hot-Wire Voltage Fluctuations (Horizontal Scale, 234 mv/in or 92.1 mv/cm) Plotted Against Radial Position in the Jet (Vertical Axis) For Several Downstream Locations; $Re_d = 3.70 \times 10^4$, $r_b = 1.04$ (Ideally Expanded Jet)

occur at the shear annulus (region of high velocity gradient at the jet edge). The flow in the jet core and exterior to the jet is fairly uniform, with low fluctuation levels. At locations further downstream in the jet, the high fluctuation shear annulus is found to thicken and converge, with the result that the peak level of RMS fluctuations is finally located approximately on the jet axis. At the location of the appearance of the maximum fluctuation level on the jet centerline, the jet may be considered fully turbulent, with dissipation decreasing the fluctuation levels in the downstream direction.

An introductory note on the behavior of trubulent jets is appropriate at this time. Nagamatsu, et al (7) carried out a fairly complete investigation of the turbulent jet. A major feature of the turbulent jet is the initially high fluctuation level in the shear annulus, with a relatively quiescent flow on the jet axis. The quiescent flow on the jet axis extends downstream for an appreciable distance (about 4 to 6 jet diameters), and corresponds to the pressence of a "potential core" in the jet. The potential core results from the fact that the high level fluctuations generated in the shear annulus spread across the jet fairly slowly. The potential core and initially high fluctuation levels in the shear annulus are important features of the turbulent jet.

Figure 9 is a plot of maximum RMS fluctuation level in the shear annulus as a function of downstream distance for the cases shown in Figures 6, 7 and 8. The plot for $Re_d = 1.23 \times 10^4$ is markedly different from the others, as the fluctuation level is initially very low, and

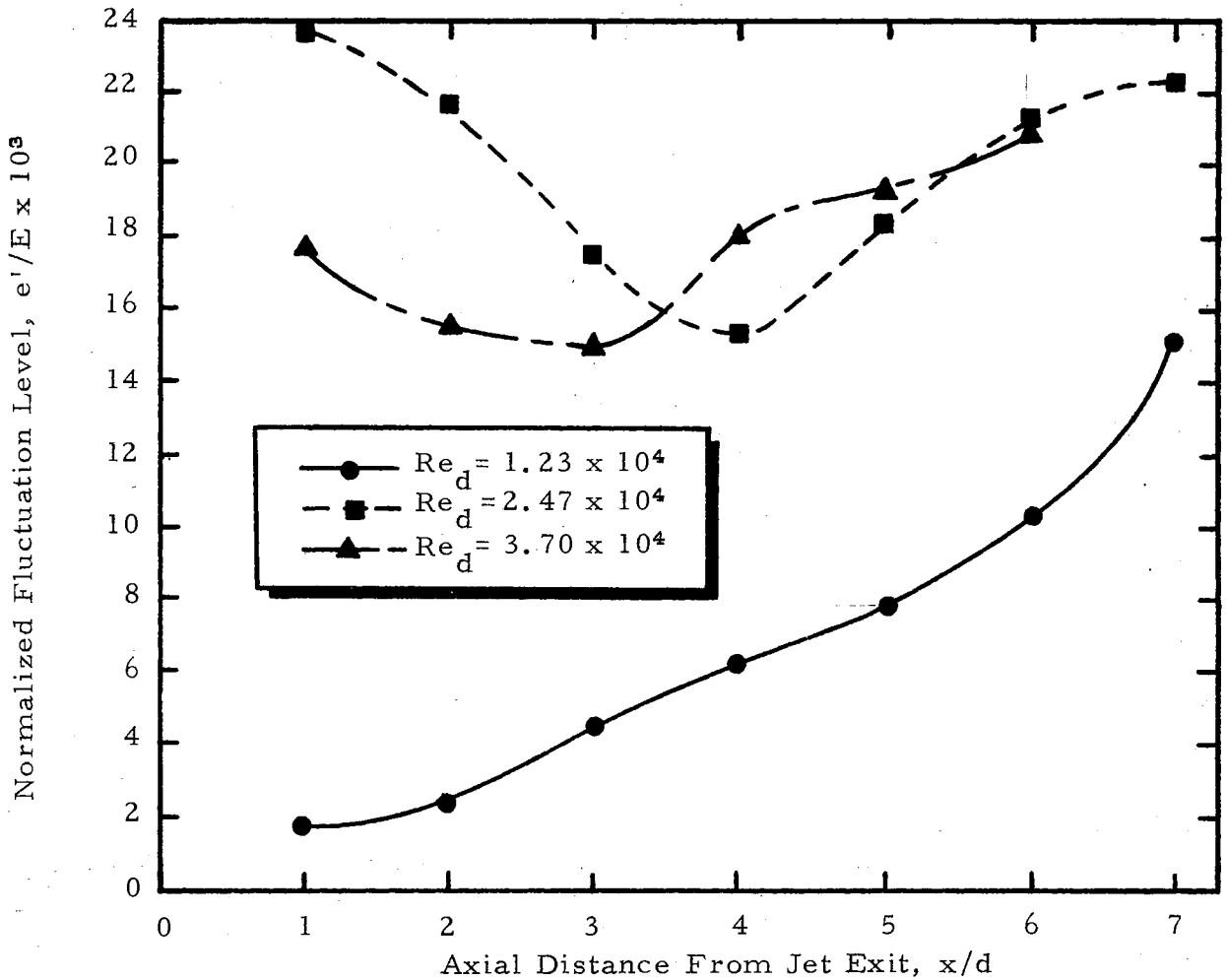

Figure 9. Maximum Normalized Fluctuation Level in the Shear Annulus as a Function of Downstream Position for the Ideally Expanded Jet at Three Reynolds Numbers

fluctuations grow at an approximately exponential rate, (exponential growth is predicted by laminar stability theory if accelerations in the streamwise direction are not large). The plots for the Reynolds numbers of 2.47×10^4 and 3.70×10^4 show behavior more consistent with that of the turbulent jet discussed previously.

In Figure 10 these observations are confirmed. This figure is a plot of RMS fluctuation level on the centerline of the jet for three Reynolds numbers. For the Reynolds numbers of 2.47×10^4 and 3.70×10^4 the presence of the potential core is indicated, but for $Re_d = 1.23 \times 10^4$ a clear difference is evident. The point of sharp increase in fluctuation level on the jet centerline occurs about two jet diameters further downstream than for the two higher Reynolds numbers.

An interesting comparison between the supersonic jet and supersonic wake flows can be made at this point. Demetriades (6) performed a hot-wire investigation to determine the spatial distribution of fluctuation amplitudes in a laminar two-dimensional supersonic wake. His results clearly show some similarities to the lowest Reynolds number jet flow (Figure 6). The wake fluctuation profiles indicate small fluctuation peaks at the shear layers for locations near the body (a wedge), with the amplitude growing in the downstream direction and with the shear layers becoming thicker. The behavior on the wake axis is similar to that shown in the jet, where initially low fluctuation amplitudes grow in the downstream direction. One must be careful not to over-interpret this comparison because of the complicating feature

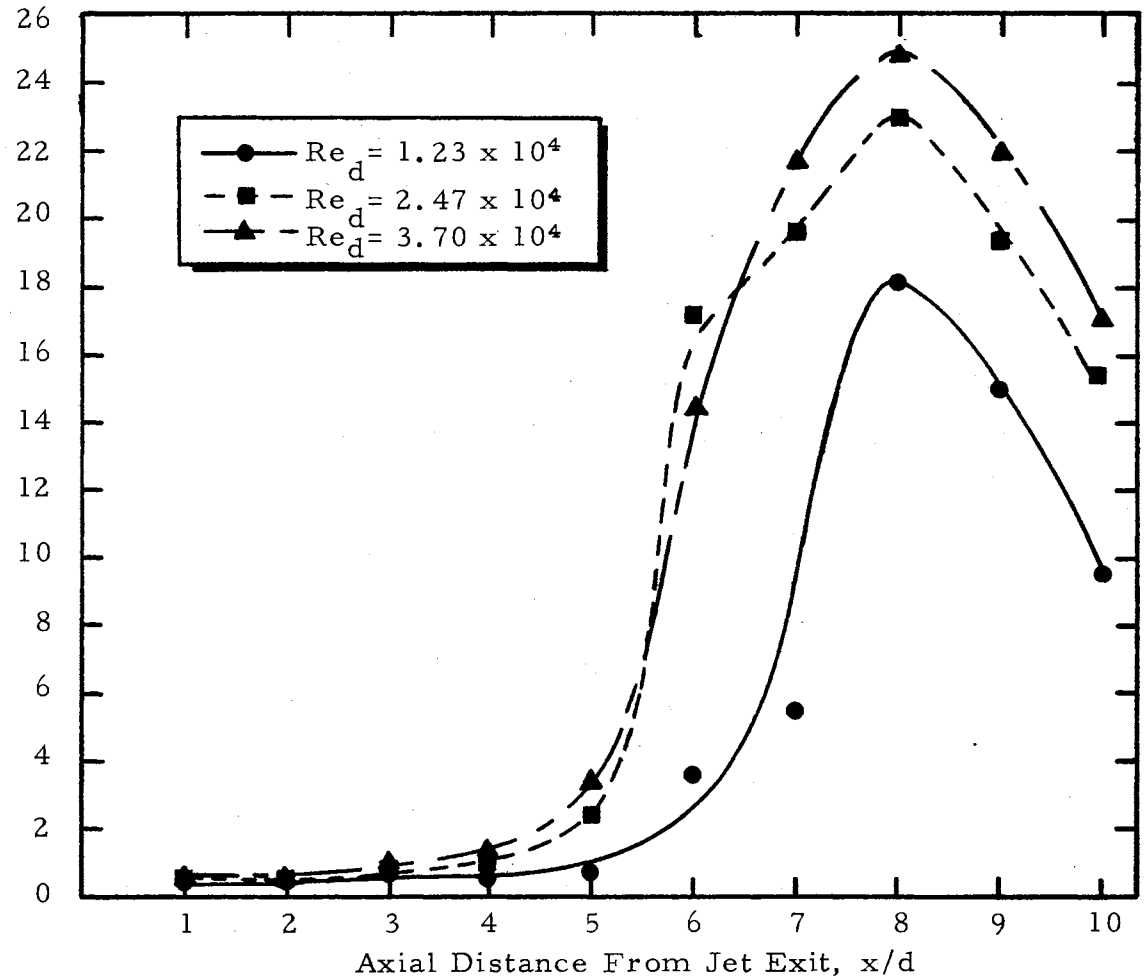

Figure 10. Normalized RMS Fluctuation Level on the Jet Centerline as a Function of Downstream Position for the Ideally Expanded Jet at Three Reynolds Numbers

of the potential core in the "fully" turbulent jet.

Since growth fluctuations (in accordance with predictions of laminar stability theory) only occurs for the case of $Re_d = 1.23 \times 10^4$, this flow is the only one which can be said to be initially laminar, and the jet should be considered turbulent for $Re_d = 2.47 \times 10^4$ and $Re_d = 3.70 \times 10^4$ from this standpoint. These conclusions are subject to further interpretation in light of information obtained from frequency spectra of the hot-wire fluctuations.

Figure 11 is a plot of the spatial distribution of RMS hot-wire voltage fluctuations for the under-expanded jet at $Re_d = 1.235 \times 10^4$. A comparison between this figure and Figure 6 indicates the effect of under-expanding the jet as far as the spatial distribution of fluctuation amplitudes is concerned. In Figure 6 (ideally expanded jet) at $x/d = 1$, small humps in the fluctuation profile may be noted near the jet axis. These correspond to weak expansion waves from the nozzle lip, and their effects die out before the downstream position $x/d = 4$ is reached. In Figure 11 (highly under-expanded case), however, a shock cell structure is formed that greatly influences the flow. The higher effective Mach number seems to increase the length from the nozzle exit before the jet is fully turbulent as compared to the ideally expanded case, but the picture is somewhat clouded by the shock structure, which increases the difficulty of drawing other meaningful conclusions. The spatial amplitude distributions for the under-expanded jet at Reynolds numbers of 2.47×10^4 and 3.70×10^4 were not included because they

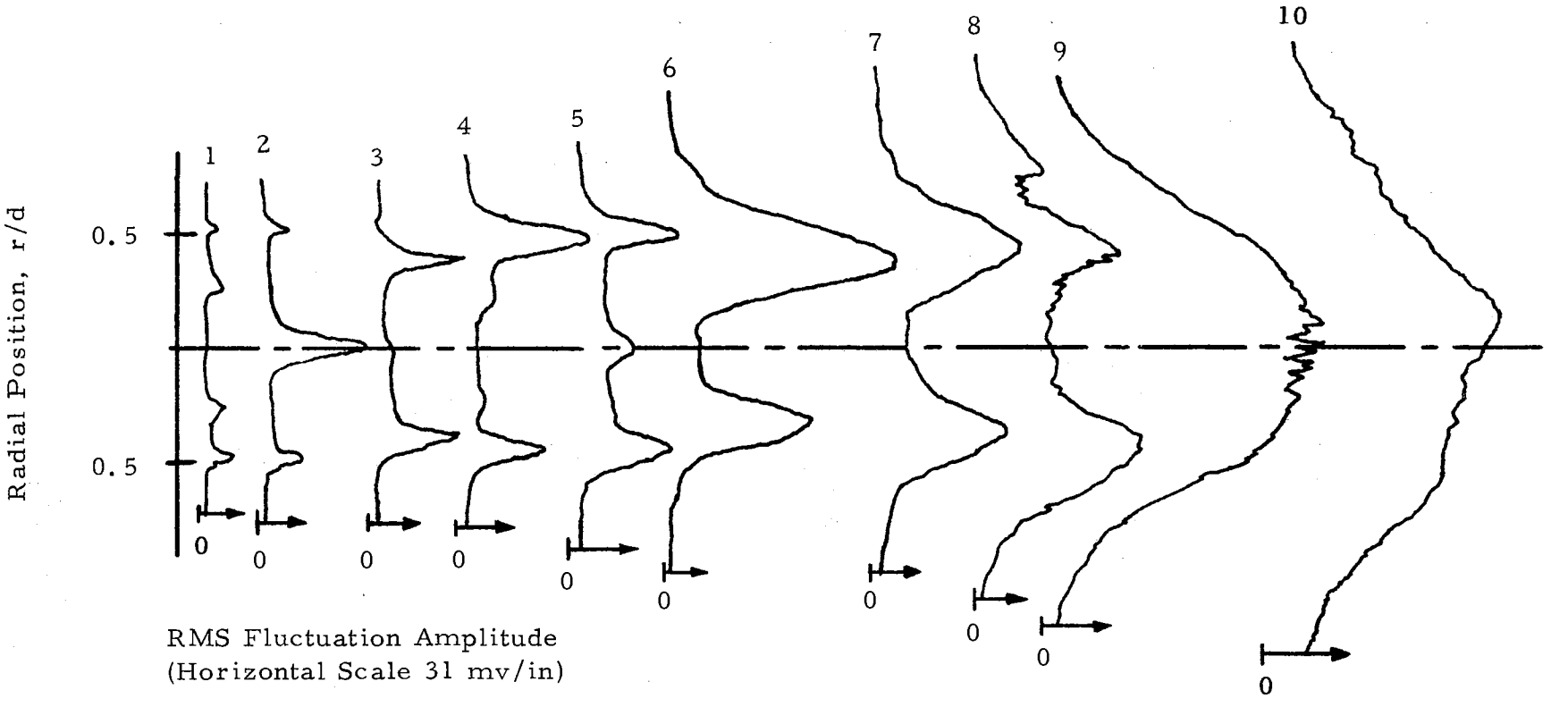

Figure 11. RMS Amplitude of Hot-Wire Voltage Fluctuations (Horizontal Scale, 31 mv/in or 12.2 mv/cm) Plotted Against Radial Position in the Jet (Vertical Axis) for Several Downstream Locations; $Re_d = 1.23 \times 10^4$, $r_b = 1.85$ (Under-Expanded Jet)

show the same effects as indicated; the point of fully turbulent flow-moves downstream about one jet diameter from that of the ideally expanded case, and the shock structure becomes evident. The other spatial behavior characteristics of the jet (spatial growth, fluctuation levels) change only slightly.

Figures 12, 13 and 14 represent frequency spectra of the hot-wire fluctuations for the ideally expanded jet at Reynolds numbers of 1.23×10^4, 2.47×10^4, and 3.7×10^4 respectively. All spectra were taken at the radial poisition of highest RMS fluctuation level in the shear annulus, with the downstream position of the probe optimized so that the best "pure tone" (as determined with the hot-wire fluctuation voltage displayed on an oscilloscope) was obtained. Features of interest in the spectra are major peaks (corresponding to oscillations of discrete frequency content) which appear far more than one Reynolds number. For example, Figure 12 indicates a discrete peak at a non-dimensional frequency of 0.182, with a harmonic at St = 0.364 (for $Re_d = 1.23 \times 10^4$). Figure 13 shows a discrete peak at 0.193, with a harmonic at 0.396 (for $Re_d = 2.47 \times 10^4$). The difference in frequency for the fundamental peaks in the two cases amounts to about 5%. This discrepancy could be caused by the difference in jet Mach number between the cases, which amounts to about 2%. Also, the frequency of the discrete oscillation may be slightly dependent on jet Reynolds number. In any case, the agreement between the frequencies of the discrete oscillations in these two cases is sufficient to support the conclusion

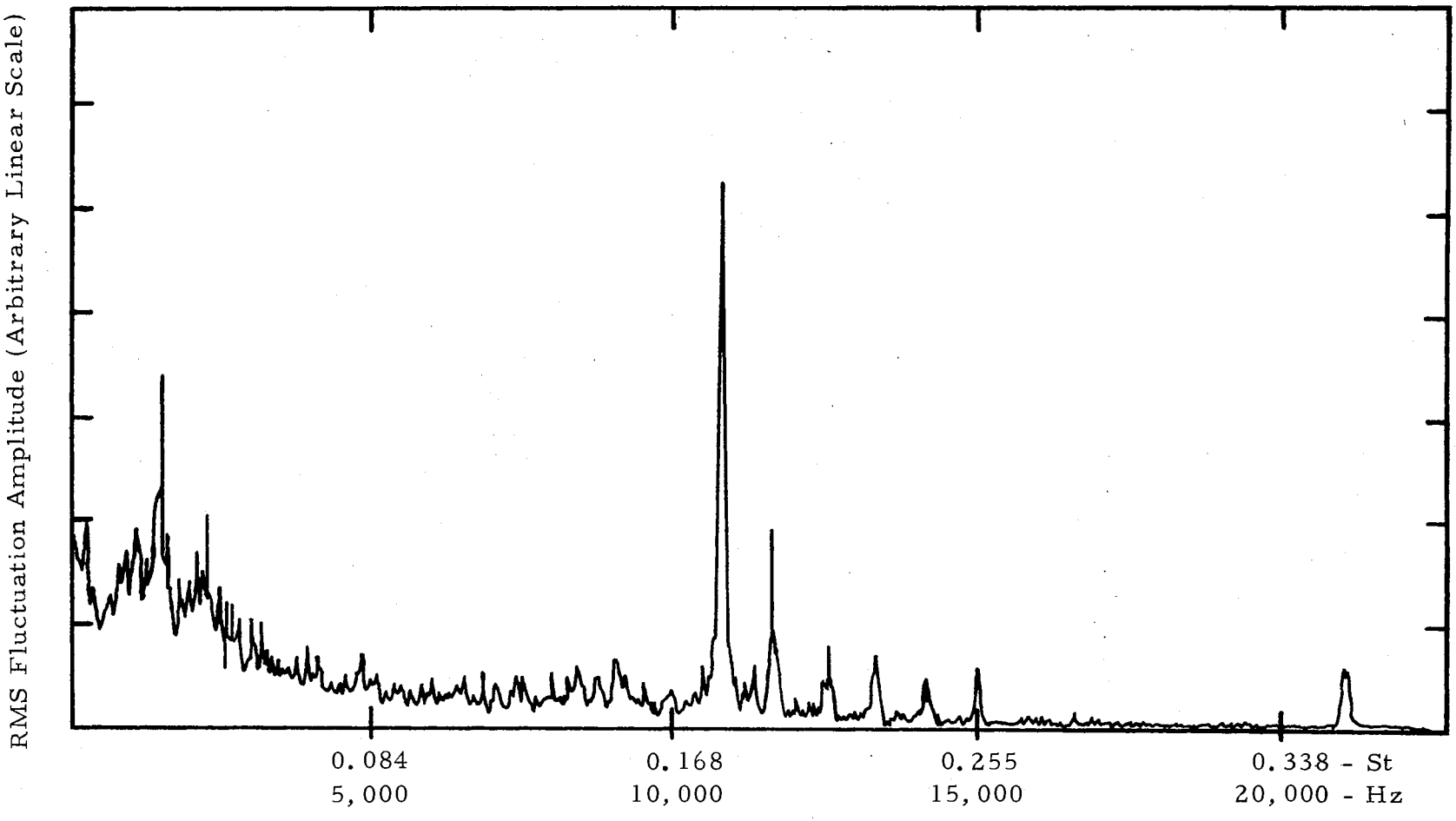

Figure 12. Frequency Spectrum of Hot-Wire Fluctuations in the Maximum Fluctuation Region of the Shear Annulus; $Re_d = 1.23 \times 10^4$, $r_b = 1.04$, $x/d = 5$, $r/d = 0.8$

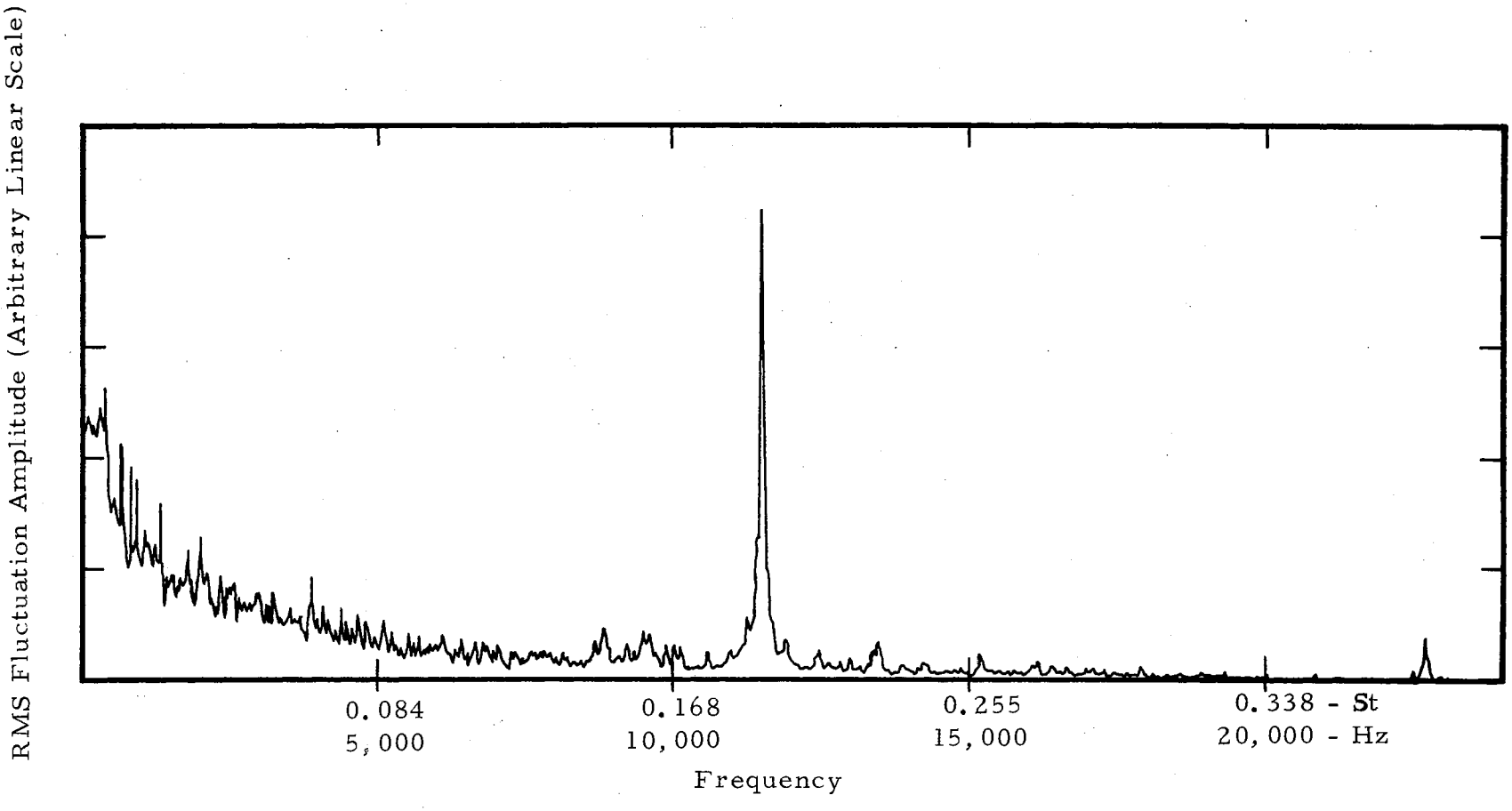

Figure 13. Frequency Spectrum of Hot-Wire Fluctuations in the Maximum Fluctuation Region of the Shear Annulus; $Re_d = 2.47 \times 10^4$, $r_b = 1.03$, $x/d = 4$, $r/d = 0.8$

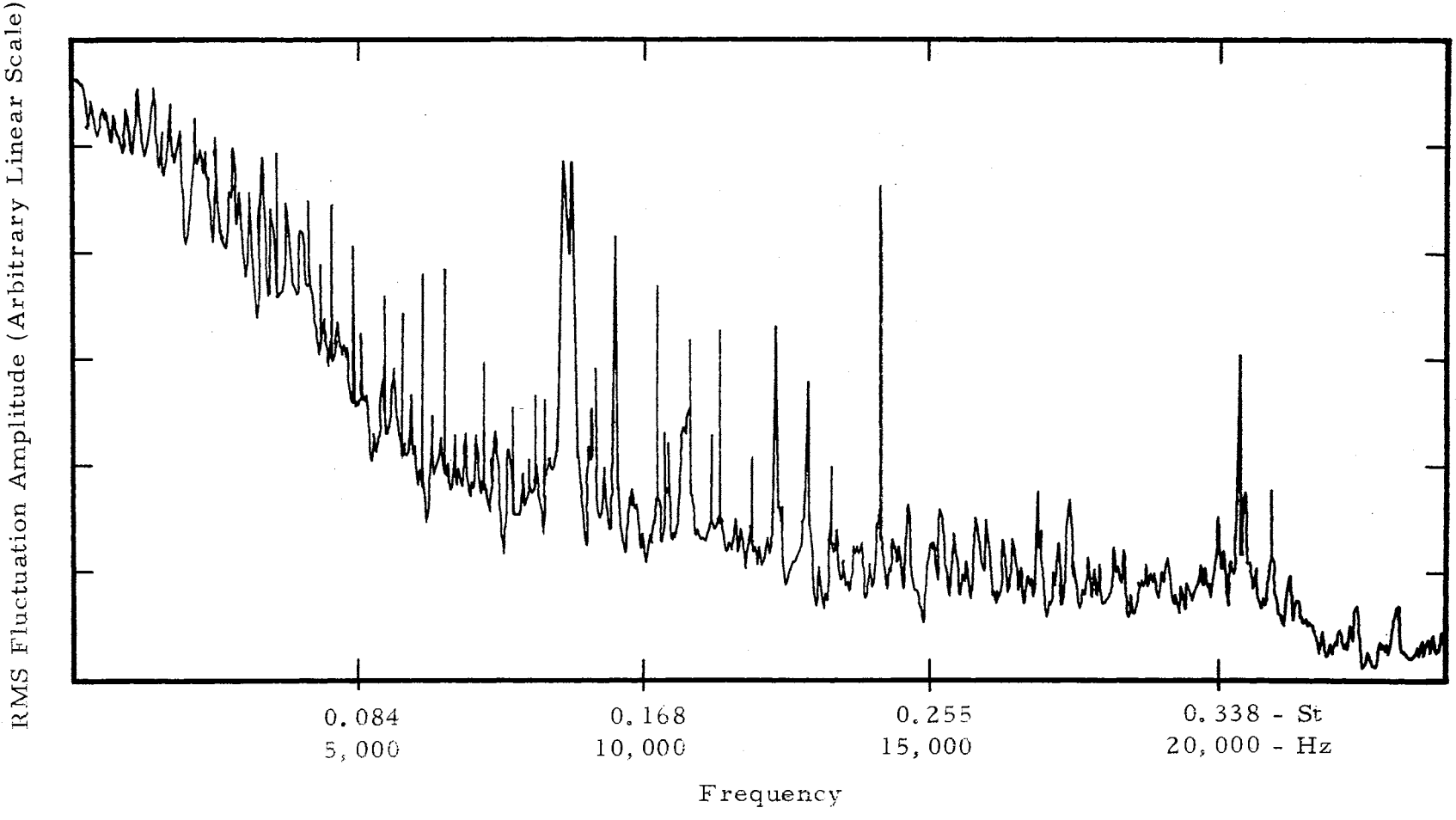

Figure 14. Frequency Spectrum of Hot-Wire Fluctuations in the Maximum Fluctuation Region of the Shear Annulus; $Re_d = 3.70 \times 10^4$, $r_b = 1.04$, $x/d = 3.5$, $r/d = 0.8$

that the same physical process is taking place at the jet Reynolds numbers of 1.23×10^4 and 2.47×10^4. For these Reynolds numbers the fluctuations in the jet are mainly due to the presence of orderly laminar instability waves in the jet. Discrete frequency instability waves have also been reported in a laminar supersonic cone wake by McLaughlin (9).

In contrast to the previously discussed cases, the spectrum for the ideally expanded jet at $Re_d = 3.70 \times 10^4$ is a rather broad-band spectrum (see Figure 14). In passing over the frequency range several times with the wave analyzer, most of the indicated "spikes" showed up only randomly. Again, a longer averaging time (or a slightly broader bandwidth) on the wave analyzer would aid in resolution of the frequency spectra, but the available information is sufficient to indicate that the peaks due to laminar instability waves are obscurred in the high Reynolds number case.

These measurements, together with the spatial amplitude distributions of the hot-wire voltage fluctuations are sufficient to determine the laminar or turbulent character of the jet. For jet Reynolds numbers of 1.23×10^4 and 2.47×10^4 a large proportion of the fluctuations in the jet occur at a single frequency. This is due to the presence of orderly waves in the jet rather than the random and chaotic fluctuations which are a characteristic of turbulence. This orderly and predictable behavior agrees with the criteria of the definition of laminar flow, and the jet is concluded to be initially laminar for Reynolds numbers of

1.23×10^4 and 2.47×10^4. This conclusion is contrary to the conclusion based on growth of fluctuations for the Reynolds number of 2.47×10^4, and indicates that both growth rates and spectra of the fluctuations should be considered in an investigation of the laminar or turbulent character of the jet flow. The flow is found to be turbulent for the Reynolds number of 3.70×10^4, with both the criteria of random fluctuations and no growth of disturbances being satisfied in this case.

Spectra of the hot-wire fluctuations in the under-expanded jet for Reynolds numbers of 1.23×10^4, 2.47×10^4 and 3.70×10^4 are presented in Figures 15, 16 and 17 respectively. The important features to be noted are that discrete peaks are shown for every Reynolds number, and that the frequencies of the discrete oscillations have been shifted from those observed in the ideally expanded jet.* For $Re_d = 1.23 \times 10^4$ the major peaks occur at St = 0.144 and St = 0.167, with an apparent harmonic at St = 0.288 for the under-expanded case (Figure 12). These compare to the peak noted at St = 0.182 and the harmonic at St = 0.364, which were mentioned for the ideally expanded jet at $Re_d = 1.23 \times 10^4$. A similar shift is observed at $Re_d = 2.47 \times 10^4$, with the major peak occurring at St = 3.70×10^4 (Figure 17) a peak is noted at St = 0.148

---

*An interesting characteristic of the shift (for $Re_d = 1.23 \times 10^4$ and 2.47×10^4) was that it occurred in a "jump" which was easily observed on an oscilloscope as the pressure balance ratio r_b was changed. For $Re_d = 3.70 \times 10^4$, where no discrete frequency fluctuations were initially present, decreasing the nozzle back pressure (increasing r_b) resulted in the sudden appearance of the discrete oscillation (also easily observed on the oscilloscope).

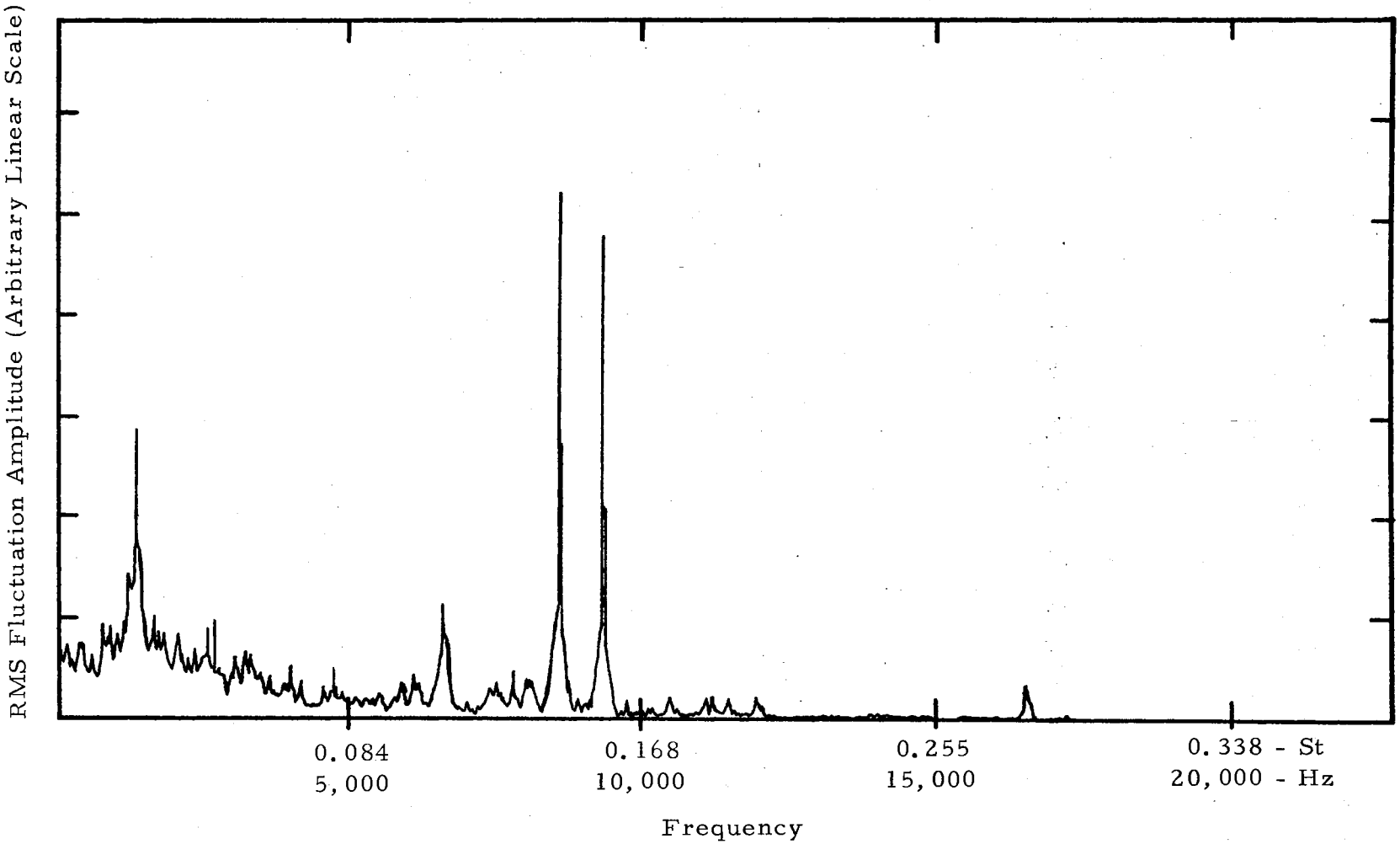

Figure 15. Frequency Spectrum of Hot-Wire Fluctuations in the Maximum Fluctuation Region of the Shear Annulus; $Re_d = 1.23 \times 10^4$, $r_b = 1.84$, $x/d = 5$, $r/d = 0.9$

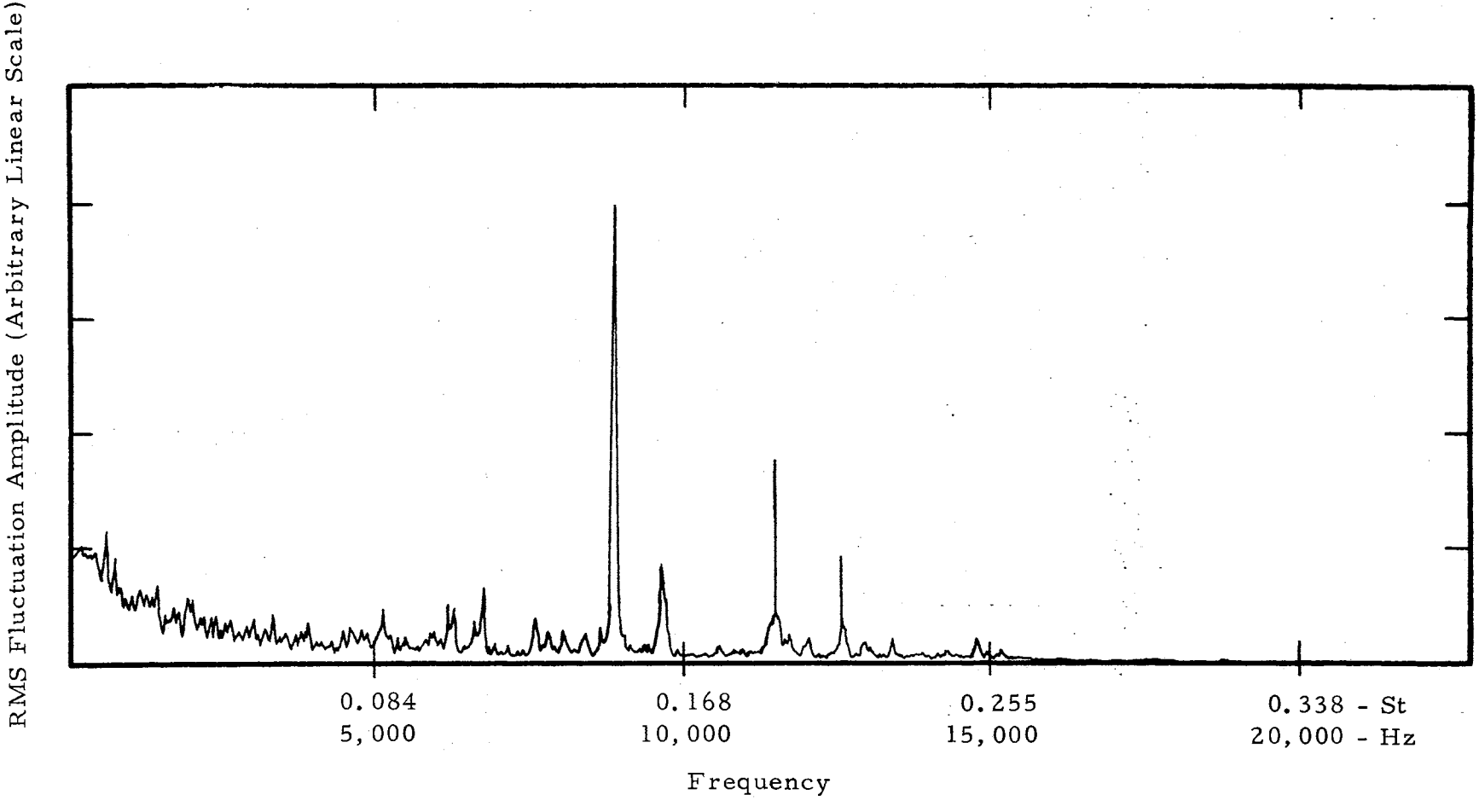

Figure 16. Frequency Spectrum of Hot-Wire Fluctuations in the Maximum Fluctuation Region of the Shear Annulus; $Re_d = 2.47 \times 10^4$, $r_b = 1.84$, $x/d = 4$, $r/d = 1.0$

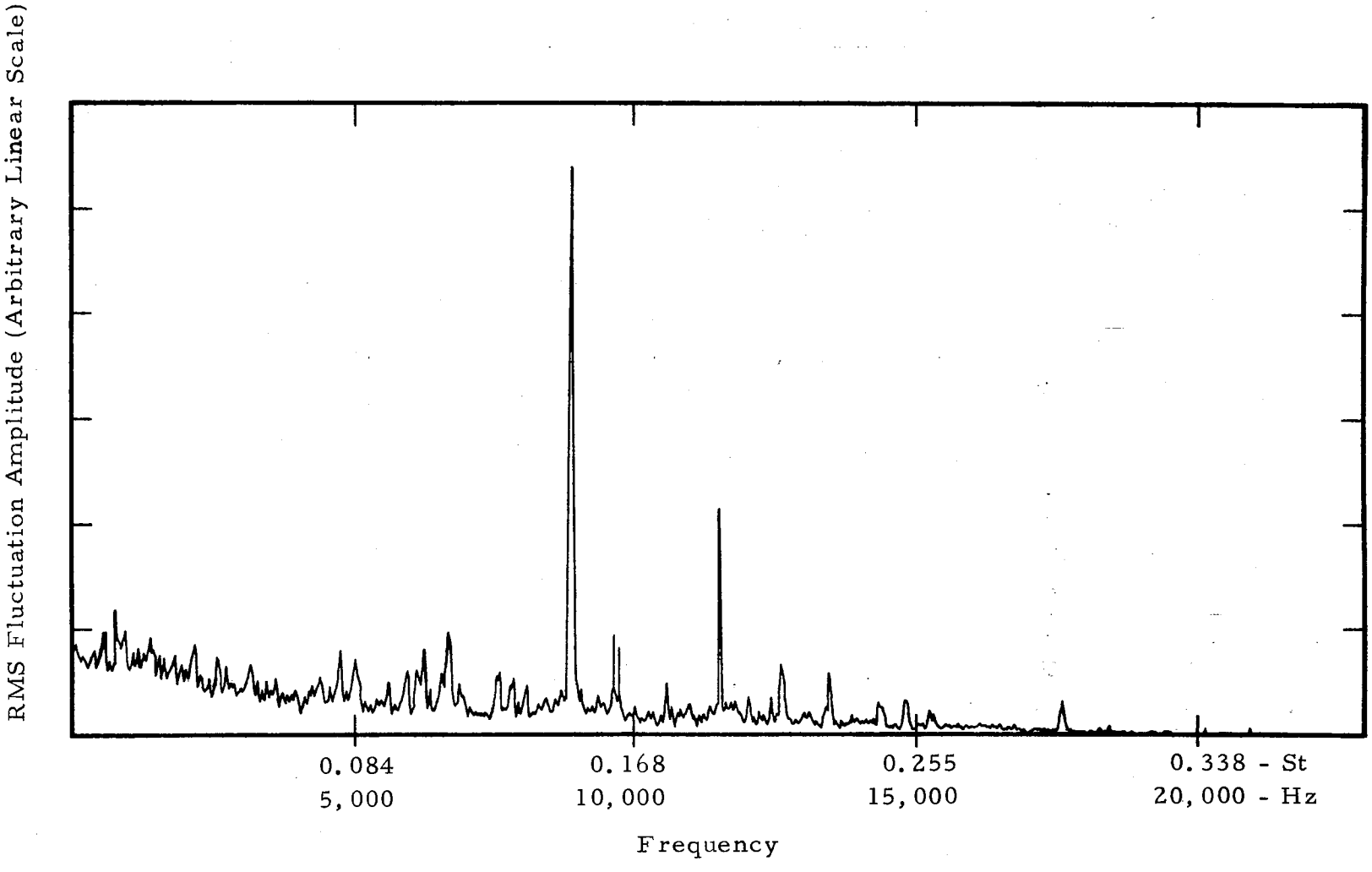

Figure 17. Frequency Spectrum of Hot-Wire Fluctuations in the Maximum Fluctuation Region of the Shear Annulus; $Re_d = 3.70 \times 10^4$, $r_b = 1.84$, $x/d = 3.5$, $r/d = 0.95$

with a harmonic at St = 0.294. The conclusion suggested by these results is that operating the jet at an off-design pressure ratio (introducing a relatively strong shock structure into the jet) may cause the inertial disturbances in the jet to "lock on" to some dimension which might be associated with the shock structure. However, this phenomenon is not completely understood at the present time.

CHAPTER IV

SUMMARY

A facility has been developed which allows control over the Reynolds number and back pressure of a free supersonic jet. The ideally expanded Mach number 2.55 jet is found to be initially laminar for Reynolds numbers of 1.23×10^4 and 2.47×10^4, and turbulent at a Reynolds number of 3.70×10^4. Under-expanding the jet stabilizes the flow for both laminar and turbulent cases, and moves the initial point of fully developed turbulence downstream about one jet diameter.

Discrete frequency instability waves are present in the ideally expanded laminar jet, but the fluctuations in the expanded turbulent jet show a broad-band spectrum. Operating the jet in an off-design pressure ratio, however, introduced discrete frequency fluctuations for all Reynolds numbers considered (with the under-expanded fundamental frequency showing a "shift" from the ideally expanded laminar fluctuation fundamental frequency).

Some similarities between the ideally expanded jet flow at $Re_d = 1.23 \times 10^4$ and laminar supersonic wakes were noted. The spatial distributions of fluctuations amplitude showed similar characteristics for the two flows, and discrete frequency fluctuations were present in

both flow situations.

Futher investigations in the jet could utilize a smaller nozzle to study the transition Reynolds number of the jet, where

$$Re_{trans} = \frac{\rho V_{jet} x_{trans}}{\mu}$$

Also, investigations of the under-expanded jet at higher Reynolds numbers might give some insight on the way in which the shock structure influences the flow. Schlieren flow visualization should be included in these investigations.

SELECTED BIBLIOGRAPHY

(1) Tam, Christopher K. W. "On the Noise of a Nearly Ideally Expanded Supersonic Jet." Journal of Fluid Mechanics, Vol. 51 (1972), 69-95.

(2) Bishop, K. A., J. E. Ffowcs Williams, and W. Smith. "On the Noise Sources of the Unsuppressed High-Speed Jet." Journal of Fluid Mechanics, Vol. 50 (1971), 21-31.

(3) Tam, Christopher K. W. "Directional Acoustic Radiation from a Supersonic Jet Generated by Shear Layer Instability." Journal of Fluid Mechanics, Vol. 46 (1971), 755-768.

(4) Demetriades, A. "An Experiment on the Stability of Hypersonic Laminar Boundary Layers." Journal of Fluid Mechanics, Vol. 7 (1960), 385-396.

(5) Demetriades, A. "Observations on the Transition Process of Two-Dimensional Supersonic Wakes." AIAA Paper No. 70-793, June, 1970.

(6) Demetriades, A. "Hot-Wire Measurements in the Hypersonic Wakes of Slender Bodies." AIAA Journal, Vol. 2, No. 2 (February, 1964), 245-250.

(7) Nagamatsu, H. T., R. E. Sheer, Jr., and E. C. Bigelow "Mean and Fluctuating Velocity Contours and Acoustic Characteristics of Subsonic and Supersonic Jets." AIAA Paper No. 72-157, January, 1972.

(8) National Advisory Committee for Aeronautics, Report 1135. "Equations, Tables and Charts for Compressible Flow." Moffett Field, California: Ames Research Staff, Ames Aeronautical Laboratory, 1953.

(9) McLaughlin, Dennis K. "Experimental Investigation of the Stability of the Laminar Supersonic Cone Wake." AIAA Journal, Vol. 9, No. 4 (April, 1971), 696-702.

VITA

Charles Jefferson McColgan

Candidate for the Degree of

Master of Science

Thesis: TRANSITION MEASUREMENTS IN A LAMINAR SUPERSONIC JET

Major Field: Mechanical Engineering

Biographical:

Personal Data: Born in Ponca City, Oklahoma, October, 1949, the son of Mr. and Mrs. C. E. McColgan.

Education: Graduated from Ponca City Senior High School in June, 1967; received the Bachelor of Science degree in Mechanical Engineering at Oklahoma State University, Stillwater, Oklahoma, in January, 1972; completed requirements for the Master of Science degree at Oklahoma State University in July, 1973.

Honors: President's Scholarship, National Merit Scholarship.

Professional Societies: American Society of Mechanical Engineers, American Institute of Aeronautics and Astronautics.